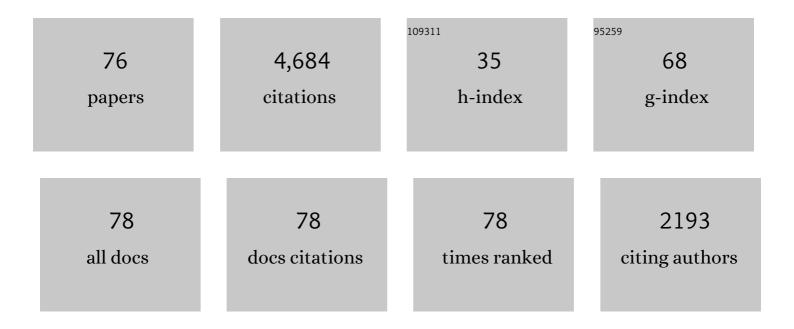
List of Publications by Year in descending order

Source: https://exaly.com/author-pdf/9180507/publications.pdf Version: 2024-02-01



SHENC-AO

#	Article	IF	CITATIONS
1	Assembly of the Lhasa and Qiangtang terranes in central Tibet by divergent double subduction. Lithos, 2016, 245, 7-17.	1.4	432
2	Magmatic record of India-Asia collision. Scientific Reports, 2015, 5, 14289.	3.3	316
3	Geochemical contrasts between early Cretaceous ore-bearing and ore-barren high-Mg adakites in central-eastern China: Implications for petrogenesis and Cu–Au mineralization. Geochimica Et Cosmochimica Acta, 2010, 74, 7160-7178.	3.9	286
4	Post-collisional granitoids from the Dabie orogen: New evidence for partial melting of a thickened continental crust. Geochimica Et Cosmochimica Acta, 2011, 75, 3815-3838.	3.9	248
5	High-precision copper and iron isotope analysis of igneous rock standards by MC-ICP-MS. Journal of Analytical Atomic Spectrometry, 2014, 29, 122-133.	3.0	159
6	Investigation of magnesium isotope fractionation during granite differentiation: Implication for Mg isotopic composition of the continental crust. Earth and Planetary Science Letters, 2010, 297, 646-654.	4.4	150
7	Magnesium Isotopic Compositions of International Geological Reference Materials. Geostandards and Geoanalytical Research, 2015, 39, 329-339.	3.1	149
8	Northward subduction of Bangong–Nujiang Tethys: Insight from Late Jurassic intrusive rocks from Bangong Tso in western Tibet. Lithos, 2014, 205, 284-297.	1.4	140
9	Zinc isotope evidence for a large-scale carbonated mantle beneath eastern China. Earth and Planetary Science Letters, 2016, 444, 169-178.	4.4	140
10	Zinc isotope fractionation during mantle melting and constraints on the Zn isotope composition of Earth's upper mantle. Geochimica Et Cosmochimica Acta, 2017, 198, 151-167.	3.9	135
11	Contrasting zircon Hf–O isotopes and trace elements between ore-bearing and ore-barren adakitic rocks in central-eastern China: Implications for genetic relation to Cu–Au mineralization. Lithos, 2013, 156-159, 97-111.	1.4	131
12	Copper isotopic composition of the silicate Earth. Earth and Planetary Science Letters, 2015, 427, 95-103.	4.4	127
13	Copper and iron isotope fractionation during weathering and pedogenesis: Insights from saprolite profiles. Geochimica Et Cosmochimica Acta, 2014, 146, 59-75.	3.9	116
14	High-temperature inter-mineral magnesium isotope fractionation in mantle xenoliths from the North China craton. Earth and Planetary Science Letters, 2011, 308, 131-140.	4.4	104
15	Zinc isotope evidence for intensive magmatism immediately before the end-Permian mass extinction. Geology, 2017, 45, 343-346.	4.4	90
16	Mg, Sr, and O isotope geochemistry of syenites from northwest Xinjiang, China: Tracing carbonate recycling during Tethyan oceanic subduction. Chemical Geology, 2016, 437, 109-119.	3.3	79
17	Copper and zinc isotope fractionation during deposition and weathering of highly metalliferous black shales in central China. Chemical Geology, 2016, 445, 24-35.	3.3	73
18	Copper isotope fractionation during adsorption onto kaolinite: Experimental approach and applications. Chemical Geology, 2015, 396, 74-82.	3.3	68

#	Article	IF	CITATIONS
19	The Cretaceous adakitic–basaltic–granitic magma sequence on south-eastern margin of the North China Craton: Implications for lithospheric thinning mechanism. Lithos, 2012, 134-135, 163-178.	1.4	66
20	Cu isotopes reveal initial Cu enrichment in sources of giant porphyry deposits in a collisional setting. Geology, 2019, 47, 135-138.	4.4	65
21	Felsic volcanism as a factor driving the end-Permian mass extinction. Science Advances, 2021, 7, eabh1390.	10.3	63
22	Compositional transition in natural alkaline lavas through silica-undersaturated melt–lithosphere interaction. Geology, 2018, 46, 771-774.	4.4	62
23	Cu and Zn isotope fractionation during oceanic alteration: Implications for Oceanic Cu and Zn cycles. Geochimica Et Cosmochimica Acta, 2019, 257, 191-205.	3.9	59
24	Copper and zinc isotope systematics of altered oceanic crust at IODP Site 1256 in the eastern equatorial Pacific. Journal of Geophysical Research: Solid Earth, 2016, 121, 7086-7100.	3.4	56
25	Copper isotope fractionation during sulfide-magma differentiation in the Tulaergen magmatic Ni–Cu deposit, NW China. Lithos, 2017, 286-287, 206-215.	1.4	53
26	Eocene magmatic processes and crustal thickening in southern Tibet: Insights from strongly fractionated ca. 43Ma granites in the western Gangdese Batholith. Lithos, 2015, 239, 128-141.	1.4	52
27	Late Jurassic sodium-rich adakitic intrusive rocks in the southern Qiangtang terrane, central Tibet, and their implications for the Bangong–Nujiang Ocean subduction. Lithos, 2016, 245, 34-46.	1.4	52
28	Tracing the Deep Carbon Cycle Using Metal Stable Isotopes: Opportunities and Challenges. Engineering, 2019, 5, 448-457.	6.7	52
29	Zircon U–Pb ages, Hf–O isotopes and trace elements of Mesozoic high Sr/Y porphyries from Ningzhen, eastern China: Constraints on their petrogenesis, tectonic implications and Cu mineralization. Lithos, 2014, 200-201, 299-316.	1.4	46
30	Iron isotopic compositions of adakitic and non-adakitic granitic magmas: Magma compositional control and subtle residual garnet effect. Geochimica Et Cosmochimica Acta, 2017, 203, 89-102.	3.9	44
31	Redox reactions control Cu and Fe isotope fractionation in a magmatic Ni–Cu mineralization system. Geochimica Et Cosmochimica Acta, 2019, 249, 42-58.	3.9	43
32	Magnesium isotopic composition of the deep continental crust. American Mineralogist, 2016, 101, 243-252.	1.9	42
33	Zn-Sr isotope records of the Ediacaran Doushantuo Formation in South China: diagenesis assessment and implications. Geochimica Et Cosmochimica Acta, 2018, 239, 330-345.	3.9	38
34	Cadmium Isotope Ratios of Standard Solutions and Geological Reference Materials Measured by <scp>MC</scp> â€ <scp>ICP</scp> â€ <scp>MS</scp> . Geostandards and Geoanalytical Research, 2018, 42, 593-605.	3.1	37
35	Magnesium isotopic heterogeneity across the cratonic lithosphere in eastern China and its origins. Earth and Planetary Science Letters, 2016, 451, 77-88.	4.4	36
36	Zinc and strontium isotope evidence for climate cooling and constraints on the Frasnian-Famennian (~372†Ma) mass extinction. Palaeogeography, Palaeoclimatology, Palaeoecology, 2018, 498, 68-82.	2.3	35

#	Article	IF	CITATIONS
37	Transition From Lowâ€K to Highâ€K Calcâ€Alkaline Magmatism at Approximately 84ÂMa in the Eastern Pontides (NE Turkey): Magmatic Response to Slab Rollback of the Black Sea. Journal of Geophysical Research: Solid Earth, 2018, 123, 7604-7628.	3.4	34
38	Origin of the Miocene porphyries and their mafic microgranular enclaves from Dabu porphyry Cu–Mo deposit, southern Tibet: implications for magma mixing/mingling and mineralization. International Geology Review, 2014, 56, 571-595.	2.1	32
39	Extreme Mg and Zn isotope fractionation recorded in the Himalayan leucogranites. Geochimica Et Cosmochimica Acta, 2020, 278, 305-321.	3.9	31
40	Antimony isotope fractionation in hydrothermal systems. Geochimica Et Cosmochimica Acta, 2021, 306, 84-97.	3.9	31
41	Copper isotope behavior during extreme magma differentiation and degassing: a case study on Laacher See phonolite tephra (East Eifel, Germany). Contributions To Mineralogy and Petrology, 2016, 171, 1.	3.1	30
42	Copper isotopic signature of the Tiegelongnan high-sulfidation copper deposit, Tibet: implications for its origin and mineral exploration. Mineralium Deposita, 2016, 51, 591-602.	4.1	30
43	Zinc Isotope Constraints on Recycled Oceanic Crust in the Mantle Sources of the Emeishan Large Igneous Province. Journal of Geophysical Research: Solid Earth, 2019, 124, 12537-12555.	3.4	30
44	Fractionation of Mg isotopes by clay formation and calcite precipitation in groundwater with long residence times in a sandstone aquifer, Ordos Basin, China. Geochimica Et Cosmochimica Acta, 2018, 237, 261-274.	3.9	29
45	Basaltic and Solution Reference Materials for Iron, Copper and Zinc Isotope Measurements. Geostandards and Geoanalytical Research, 2019, 43, 163-175.	3.1	29
46	Mg and Zn Isotope Evidence for Two Types of Mantle Metasomatism and Deep Recycling of Magnesium Carbonates. Journal of Geophysical Research: Solid Earth, 2020, 125, e2020JB020684.	3.4	29
47	Generation of leucogranites via fractional crystallization: A case from the Late Triassic Luoza batholith in the Lhasa Terrane, southern Tibet. Gondwana Research, 2019, 66, 63-76.	6.0	28
48	The fate of subducting carbon tracked by Mg and Zn isotopes: A review and new perspectives. Earth-Science Reviews, 2022, 228, 104010.	9.1	27
49	Calibrating NIST SRM 683 as a new international reference standard for Zn isotopes. Journal of Analytical Atomic Spectrometry, 2018, 33, 1777-1783.	3.0	26
50	Zinc, cadmium and sulfur isotope fractionation in a supergiant MVT deposit with bacteria. Geochimica Et Cosmochimica Acta, 2019, 265, 1-18.	3.9	25
51	Contrasting zinc isotopic fractionation in two mafic-rock weathering profiles induced by adsorption onto Fe (hydr)oxides. Chemical Geology, 2020, 539, 119504.	3.3	25
52	Evolution of Intraplate Alkaline to Tholeiitic Basalts via Interaction Between Carbonated Melt and Lithospheric Mantle. Journal of Petrology, 2021, 62, .	2.8	25
53	The origin and evolution of low-δ18O magma recorded by multi-growth zircons in granite. Earth and Planetary Science Letters, 2013, 373, 233-241.	4.4	23
54	Geochronology and geochemistry of leucogranites from the southeast margin of the North China Block: Origin and migration. Gondwana Research, 2014, 26, 1111-1128.	6.0	23

#	Article	IF	CITATIONS
55	Zinc isotope fractionation between Cr-spinel and olivine and its implications for chromite crystallization during magma differentiation. Geochimica Et Cosmochimica Acta, 2021, 313, 277-294.	3.9	23
56	Zinc isotopic compositions of migmatites and granitoids from the Dabie Orogen, central China: Implications for zinc isotopic fractionation during differentiation of the continental crust. Lithos, 2019, 324-325, 454-465.	1.4	20
57	Copper isotopic compositions of the Zijinshan high-sulfidation epithermal Cu–Au deposit, South China: Implications for deposit origin. Ore Geology Reviews, 2017, 83, 191-199.	2.7	18
58	Copper and zinc isotope fractionation during deposition and weathering of highly metalliferous black shales in central China. Chemical Geology, 2016, 422, 82.	3.3	17
59	Zinc isotopic behavior of mafic rocks during continental deep subduction. Geoscience Frontiers, 2021, 12, 101182.	8.4	16
60	Oxidation of the deep big mantle wedge by recycled carbonates: Constraints from highly siderophile elements and osmium isotopes. Geochimica Et Cosmochimica Acta, 2021, 295, 207-223.	3.9	15
61	Contrasting fates of subducting carbon related to different oceanic slabs in East Asia. Geochimica Et Cosmochimica Acta, 2022, 324, 156-173.	3.9	15
62	Highâ€Precision Measurement of Stable Cr Isotopes in Geological Reference Materials by a Doubleâ€Spike TIMS Method. Geostandards and Geoanalytical Research, 2019, 43, 647-661.	3.1	11
63	Probing recycled carbonate in the lower mantle. National Science Review, 2022, 9, .	9.5	11
64	Temporal and Spatial Variations of Enriched Source Components in Linzizong Volcanic Succession, Tibet, and Implications for the India–Asia Collision. Journal of Petrology, 2022, 63, .	2.8	11
65	Copper isotope evidence for a Cu-rich mantle source of the world-class Jinchuan magmatic Ni-Cu deposit. American Mineralogist, 2022, 107, 673-683.	1.9	10
66	Tracing carbonate dissolution in subducting sediments by zinc and magnesium isotopes. Geochimica Et Cosmochimica Acta, 2022, 319, 56-72.	3.9	10
67	Linking deep CO2 outgassing to cratonic destruction. National Science Review, 2022, 9, .	9.5	9
68	Zinc isotope evidence for carbonate alteration of oceanic crustal protoliths of cratonic eclogites. Earth and Planetary Science Letters, 2022, 580, 117394.	4.4	8
69	Carbonated Big Mantle Wedge Extending to the NE Edge of the Stagnant Pacific Slab: Constraints from Late Mesozoic-Cenozoic Basalts from Far Eastern Russia. Journal of Earth Science (Wuhan, China), 2022, 33, 121-132.	3.2	7
70	Chromium isotope fractionation during magmatic processes: Evidence from mid-ocean ridge basalts. Geochimica Et Cosmochimica Acta, 2022, 327, 79-95.	3.9	7
71	Molybdenum isotope tracing petrogenesis of adakitic rocks and associated ore-forming process. Geochimica Et Cosmochimica Acta, 2021, 300, 296-317.	3.9	6
72	Copper Isotope Fractionation during Basalt Leaching at 25 ŰC and pH = 0.3, 2. Journal of Earth Science (Wuhan, China), 2022, 33, 82-91.	3.2	6

#	Article	IF	CITATIONS
73	Magnesium and zinc isotopic anomaly of Cenozoic lavas in central Myanmar: Origins and implications for deep carbon recycling. Lithos, 2021, 386-387, 106011.	1.4	5
74	Cu and Zn Isotopic Evidence for the Magnitude of Organic Burial in the Mesoproterozoic Ocean. Journal of Earth Science (Wuhan, China), 2022, 33, 92-99.	3.2	4
75	Zinc isotopic systematics of the Mt. Baekdu and Jeju Island intraplate basalts in Korea, and implications for mantle source lithologies. Lithos, 2022, 416-417, 106659.	1.4	4
76	Initial Cu enrichment in sources of giant porphyry deposits revealed by Cu isotopes. Acta Geologica Sinica, 2019, 93, 255-256.	1.4	0